Path integral Monte Carlo study of the interacting quantum double-well model: Quantum phase transition and phase diagram

Dong-Hee Kim
Department of Physics, Korea Advanced Institute of Science and Technology, Daejeon 305-701, Republic of Korea

Yu-Cheng Lin and Heiko Rieger
Theoretische Physik, Universität des Saarlandes, 66041 Saarbrücken, Germany

(Received 17 August 2006; published 10 January 2007)

The discrete time path integral Monte Carlo with a one-particle density matrix approximation is applied to study the quantum phase transition in the coupled double-well chain. To improve the convergence properties, the exact action for a single particle in a double-well potential is used to construct the many-particle action. The algorithm is applied to the interacting quantum double-well chain for which the zero-temperature phase diagram is determined. The quantum phase transition is studied via finite-size scaling, and the critical exponents are shown to be compatible with the classical two-dimensional Ising universality class—not only in the order-disorder limit (deep potential wells), but also in the displacive regime (shallow potential wells).

DOI: 10.1103/PhysRevE.75.016702 PACS number(s): 02.70.Ss, 05.70.Fh

I. INTRODUCTION

The two-level tunneling model provides a phenomenological description of the low-temperature properties of glassy materials [1]. In the simplest case, an isolated tunneling system can be represented by a particle moving in a double-well potential. Experimental findings have suggested that the interactions between the tunneling systems play a crucial role in the low-temperature behavior which deviates from the predictions of the noninteracting two-level systems [2]. The model Hamiltonian of the system with L particles is then given by

$$\mathcal{H} = \sum_{i=1}^{L} \left(\frac{p_i^2}{2\mu} + U(x_i) \right) + \sum_{j<i} V(x_i, x_j), \tag{1}$$

where x_i is the (one-dimensional) displacement of the ith particle ($i=1,\ldots,L$) of mass μ from a reference position, $p_i = \frac{\hbar}{i}\frac{\partial}{\partial x_i}$ denotes the momentum operator, $U(x_i)$ is a local potential for the displacement of the ith particle that is usually assumed to be a double-well potential, and $V(x_i,x_j)$ describes the interaction between particles; see Fig. 1. Apart from glassy materials, this coupled double-well model has been applied to other systems, including structural phase transitions of a wide range of systems—e.g., uniaxial ferroelectrics [3]. Most numerical computations devoted to understanding the interacting double-well model have mainly treated the problem in the framework of the classical ϕ^4 model or have been limited in the "two-state" limit by studying the corresponding Ising model. These simplifications reveal the difficulties inherent in simulations of the quantum coupled double-well model.

In this paper we present an efficient path integral Monte Carlo (PIMC) algorithm to study interacting particles, each of which is confined to a double-well potential. The method is presented in the next section, and it is applied to the one-dimensional interacting double-well model in the Sec. III, which also contains the results: the phase diagram and the discussion of the universality class of the quantum phase transition.

II. THE METHOD

The partition function of Eq. (1) is given by

$$\mathcal{Z} = \int d\mathbf{x} \rho(\mathbf{x},\mathbf{x};\beta), \tag{2}$$

where $\mathbf{x}=(x_1,\ldots,x_L)$ is the displacement configuration of the whole system and

$$\rho(\mathbf{x},\mathbf{x}';\beta) = \langle \mathbf{x}|e^{-\beta\mathcal{H}}|\mathbf{x}'\rangle \tag{3}$$

is the density matrix, with $\beta=1/T$ the inverse temperature. Observables that are diagonal in the displacements, like the the mth moment $\langle x_i^m \rangle$, are given by

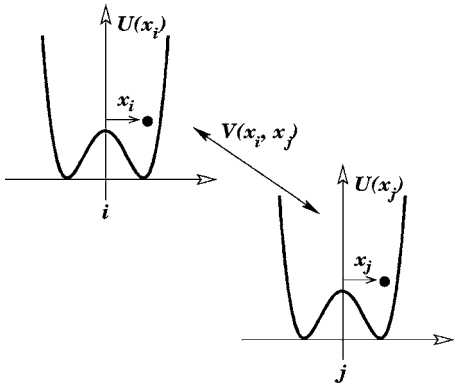

FIG. 1. Schematic representation of a coupled tunneling model in which the local potential is described by a double-well form.

 ©2007 The American Physical Society

$$\langle O(\mathbf{x})\rangle = \frac{1}{\mathcal{Z}} \int d\mathbf{x}\rho(\mathbf{x},\mathbf{x};\beta)O(\mathbf{x}). \tag{4}$$

By splitting the Hamiltonian (1) into two (noncommuting) parts $\mathcal{H}=\mathcal{H}_A+\mathcal{H}_B$ and using the Suzuki-Trotter identity, one arrives at the path integral formula for ρ:

$$e^{-\beta(\mathcal{H}_A+\mathcal{H}_B)} = \lim_{M\to\infty} [e^{-\tau\mathcal{H}_A}e^{-\tau\mathcal{H}_B}]^M, \tag{5}$$

with $\tau=\beta/M$. The conventional choice for $\mathcal{H}_A$ and $\mathcal{H}_B$ is the kinetic energy for $\mathcal{H}_A$ (which is diagonal in the momenta p_i) and the potential plus interaction energy $U+V$ for $\mathcal{H}_B$ (which is diagonal in the displacement variables). In the lowest order of the commutator expansion—the so-called primitive approximation—the high-temperature density matrix becomes

$$\rho(\mathbf{x},\mathbf{x}';\tau) = \prod_{i,j}^{L} e^{-\tau[U(x_i)+V(x_i,x_j)]/2}\rho_0(x_i,x_i';\tau)e^{-\tau[U(x_i')+V(x_i',x_j')]/2}, \tag{6}$$

where $\rho_0(x_i,x_i';\tau)$ is the free-particle density matrix. This choice leads to bad convergence properties in the Trotter number M [4] because of the fractal character of a trajectory of a free quantum mechanical particle described by the term $\mathcal{H}_A$.

The purpose of this paper is to demonstrate the efficiency of another choice for $\mathcal{H}_A$ and $\mathcal{H}_B$ by treating the single-particle diffusion within a double-well potential exactly and separately from the particle interactions. Doing this, we have

$$\mathcal{H}_A = \sum_{i=1}^{L} \frac{p_i^2}{2\mu} + U(x_i),$$

$$\mathcal{H}_B = \sum_{i<j} V(x_i,x_j). \tag{7}$$

This strategy is expected to be most promising in the case when the interactions are much weaker than the mean potential energy of the particle.

With Eqs. (7) the path integral expression for the density matrix becomes

$$\rho(\mathbf{x},\mathbf{x};\beta) = \lim_{M\to\infty} \int d\mathbf{x}_1 \cdots d\mathbf{x}_{M-1} \prod_{m=0}^{M-1} \rho_A(\mathbf{x}_m,\mathbf{x}_{m+1};\tau) \times \rho_B(\mathbf{x}_m,\mathbf{x}_{m+1};\tau), \tag{8}$$

with $\mathbf{x}=\mathbf{x}_0=\mathbf{x}_M$ and

$$\rho_A(\mathbf{x},\mathbf{x}';\tau) = \prod_{i=1}^{L} \rho^{(1)}(x_i,x_i';\tau),$$

$$\rho_B(\mathbf{x},\mathbf{x}';\tau) = \prod_{i<j} e^{-\tau[V(x_i,x_j)+V(x_i',x_j')]/2}, \tag{9}$$

where

$$\rho^{(1)}(x,x';\tau) = \langle x|e^{-\tau p^2/2\mu}|x'\rangle e^{-\tau[U(x)+U(x')]/2} \tag{10}$$

is the one-particle density matrix for a single particle in a potential U. For a double-well potential this is not known analytically but can easily be computed numerically with the matrix multiplication method [5]. This method is based on the recursion formula

$$\rho^{(1)}(x,x';2\delta\tau) = \int_{x_{\min}}^{x_{\max}} dx''\rho^{(1)}(x,x'';\delta\tau)\rho^{(1)}(x'',x';\delta\tau) \tag{11}$$

and the fact that in the limit $\delta\tau\to 0$ the one-particle density matrix $\rho^{(1)}$ can be factorized into the kinetic and potential energy parts:

$$\rho^{(1)}(x,x'';\delta\tau) \to \left(\frac{\mu}{2\pi\hbar^2\delta\tau}\right)^{1/2} e^{-\mu(x-x')^2/2\hbar^2\delta\tau}e^{-\delta\tau[U(x)+U(x')]/2}. \tag{12}$$

By squaring the density matrix k times, we will lower the temperature by a factor of 2^k and reach the required temperature τ. For a given potential $U(x)$, the limits of integration, $x_{\min}$ and $x_{\max}$, are chosen appropriately—not too large for computational reasons and not too small for numerical accuracy. Once the limits are set, a fine grid between $x_{\min}$ and $x_{\max}$ should be constructed for the numerical integrations. The spacing between successive grid points should be sufficiently small to ensure high accuracy. We store this one-particle density matrix in a two-dimensional array as a look-up table for use during the simulations and employ a simple bilinear interpolation to determine the matrix elements for any point (x_i,x_i') within $[x_{\min},x_{\max}]$ in the continuous position space. We note that the symmetric breakup of the propagator in the form of Eq. (10) satisfies a unitarity condition $\rho^{(1)}(\delta\tau)\rho^{(1)}(-\delta\tau)=1$, which can be utilized to reduce errors resulting from discretization of τ, as discussed in [6].

Path integral Monte Carlo method means the evaluation of the integral (8) via importance sampling of the configurations $(\mathbf{x}_1,\ldots,\mathbf{x}_{M-1})$ (for fixed M) with the appropriate weight given by the integrand of (8). Here we use a single-step update scheme: Let $\mathbf{X}=(\mathbf{x}_1,\ldots,\mathbf{x}_{M-1})=\{x_{i,m}\}$ be the current configuration. We generate a new configuration $\mathbf{X}'$ which differs from the old configuration $\mathbf{X}$ only in a single-particle displacement in a particular time slice: $x_{i,m}'=x_{i,m}+\delta$, where $\delta\in[-\varepsilon,\varepsilon]$ is a uniformly distributed random number and ε the step size. The acceptance probability $w(\mathbf{X}\to\mathbf{X}')$ of this new configuration should be chosen to fulfill detailed balance with respect to the weights of of the old and new configurations; a possible choice is

$$w(\mathbf{X}\to\mathbf{X}') = \min\left[1, \prod_{m=0}^{M-1} \frac{\rho_A(\mathbf{x}_{m-1},\mathbf{x}'_m;\tau)\rho_B(\mathbf{x}'_m,\mathbf{x}_{m+1};\tau)}{\rho_A(\mathbf{x}_{m-1},\mathbf{x}_m;\tau)\rho_B(\mathbf{x}_m,\mathbf{x}_{m+1};\tau)}\right]$$
$$= \min\left[1, e^{-\tau\Delta V(\mathbf{X},\mathbf{X}')} \cdot \frac{\rho^{(1)}(x_{i,m-1},x'_{i,m};\tau)\rho^{(1)}(x'_{i,m},x_{i,m+1};\tau)}{\rho^{(1)}(x_{i,m-1},x_{i,m};\tau)\rho^{(1)}(x_{i,m},x_{i,m+1};\tau)}\right]. \quad (13)$$

III. ONE-DIMENSIONAL MODEL AND RESULTS

To test the above algorithm we focus here on a one-dimensional geometry in which particles interact only with their nearest neighbors and assume $V(x_i,x_{i+1})$ to be quadratic in the displacements:

$$\mathcal{H}_B = \sum_{i<j} V(x_i,x_j) = -\sum_{i=1}^{L} J_i x_i x_{i+1} \quad (14)$$

(cf. Fig. 2). Furthermore, we choose homogeneous interaction strength $J_i=J>0$ and the double-well potential in the symmetrical form with two minima located at ±1:

$$U(x) = V_0(x^4 - 2x^2). \quad (15)$$

Periodic boundary conditions are imposed.

The model (1) with (14) and (15) has a Z_2 symmetry ($x_i \to -x_i \forall i$) and corresponds to a quantum version of a ϕ^4 theory, which is expected to belong to the universality class of (1+1)-dimensional Ising models. Suppose that the height of the potential barrier V_0 is large compared to the energy scale of the particle executing small oscillations in one of the double wells. The model is then equivalent to the one-dimensional Ising model in a transverse field:

$$\mathcal{H}_{\mathrm{TIM}} = -\Gamma\sum_i \sigma_i^x - J\sum_{\langle i,j\rangle} \sigma_i^z\sigma_j^z, \quad (16)$$

where the transverse field Γ corresponds to the tunneling splitting in the double-well problem. Therefore we expect it to display a zero-temperature quantum phase transition [9] from a disordered phase with $\langle x_i\rangle=0$ to an ordered phase with $\langle x_i\rangle\neq 0$ at a critical interaction strength J_c (for fixed μ and V_0). According to the universality hypothesis, the same universality class—i.e. the 2D Ising class—should extentd to the region where V_0 is small compared to the interactions between particles, the so-called displacive region [3,7,8].

For a given value of the parameters V_0 and J we computed the following quantities: the average of the displacement m (i.e., the magnetization in the spin formulation), defined as $m(L,M)=\frac{1}{LM}\Sigma_i^L\Sigma_n^M\langle x_{i,n}\rangle$, where $x_{i,n}$ is the position of the ith particle at the time step n with respect to the zero position of the local potential V_{dw}; the fourth-order cumulant of the magnetization given by $g=\frac{1}{2}(3-\langle m^4\rangle/\langle m^2\rangle^2)$, where $\langle\cdots\rangle$ denotes the expectation value over MC configurations; the susceptibility defined as $\chi=L\beta(\langle m^2\rangle-\langle|m|^2\rangle)$. Close to a quantum critical point, one expects [9] observables $\mathcal{O}$ to scale as

$$\mathcal{O} = L^{-x_\mathcal{O}}\tilde{O}\left(\delta L^{1/\nu}, \frac{\beta}{L^z}\right) \quad (17)$$

where $x_\mathcal{O}$ is the scaling dimension of the observable $\mathcal{O}$, ν the correlation length exponent, and z the dynamical exponent. If the transition falls into the Ising universality class, the dynamical exponent z is unity [9]. In the following we assume this to be the case and check whether our data are compatible with this. We choose a fixed value of the aspect ratio L/β, corresponding to $z=1$, so that the finite-size scaling function of these quantities involves only one variable—i.e., $\mathcal{O}=L^{-x_\mathcal{O}}\tilde{O}(\delta L^{1/\nu})$. For a given V_0, the deviation from the critical point is parametrized as $\delta=J-J_c$. The scaling dimension is given by $x_m=-\beta_m/\nu$ for the magnetization $|m|$, $x_\chi=\gamma/\nu$ for the magnetic susceptibility χ, and $x_g=0$ for the dimensionless fourth cumulant g. Typically we executed 10^6-10^7 MC steps to thermalize the system. Once in equilibrium, we generated $4-5\times10^7$ MC configurations for measurements, which were carried out every 5 MC steps. We have considered a wide rage of values of V_0 between 0.01 and 5. At a fixed value of V_0 we varied the strength of the ferromagnetic interaction J for system sizes up to $L=64$ to localize the zero-temperature critical point J_c and to carry out the finite-size analysis.

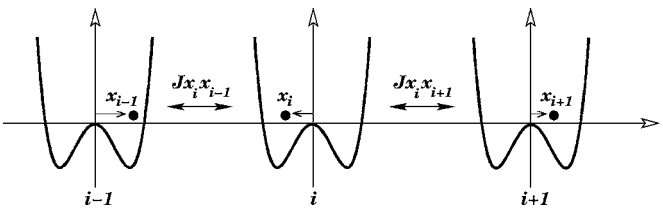

FIG. 2. Representation of the model defined in Eq. (1) in the one-dimensional form.

To confirm the accuracy of the one-particle density matrices calculated by matrix multiplication method, we first compare the distribution of displacements of the particles in the absence of the interaction obtained by PIMC with the distribution calculated by solving numerically the single-particle Schrödinger equations. For the latter, we calculated the first $N=50$ energy eigenvalues E_n and the corresponding eigenstates $\psi_n(x)$; the distribution function of the displacement is then computed by $P(x)=\Sigma_{n=1}^N|\psi_n(x)|^2e^{-\beta E_n}/\Sigma_{n=1}^N e^{-\beta E_n}$. As shown in Fig. 3 for $\beta=16$ by using $\tau=0.25$, the excellent agreement confirms the accuracy of the density matrices. Furthermore, we compare the results from the PIMC simulation within the one-particle density matrix approximation with those in the primitive approximation for the same parameters (e.g., V_0 and J), as shown in Fig. 4 as a typical example for the dependence of magnetization $|m|$ and its

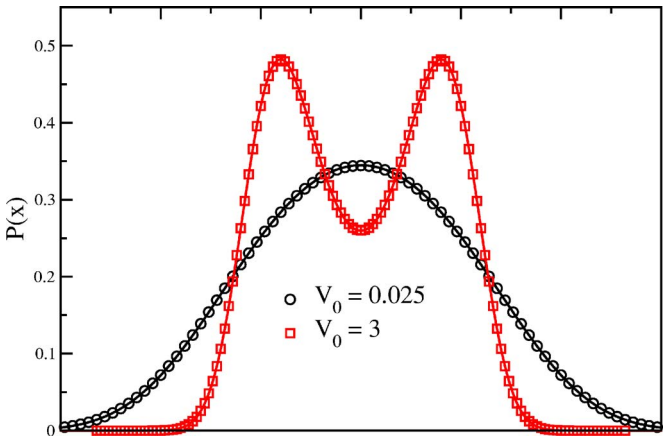

FIG. 3. (Color online) The distribution of displacements of the particles, calculated for $L=32$ and $\beta=16$, with $J=0$. A comparison with numerical solutions (indicated by the solid line) of the Schrödinger equation is shown. The excellent agreement confirms the accuracy of the density matrices.

fourth-order cumulant g on the time step τ. The results presented are averaged over 16 samples for each time step. We find that, with $\tau=0.05$, the results obtained by the primitive approximation converge to the same values computed with the one-particle density matrix for $\tau \leqslant 0.25$ within the statistical error bars. The CPU time required on an Intel Pentium processor (2.40 GHz) to calculate 500 000 MC steps for a system size $L=32$ and $\beta=16$ within the one-particle density matrix approximation using $\tau=0.25$ is about 780 s and with the primitive approximation using $\tau=0.05$ is about 1485 sec. The efficiency of the calculations with the one-particle density matrix is gained from the fast convergence with respect to the number of time slices. After a careful examination, we are convinced that the time step $\tau=0.25$, used in our simulations for the high-temperature one-particle density matrix, is sufficiently small for the convergence. We carried out eight iterations for the matrix multiplication to generate a one-

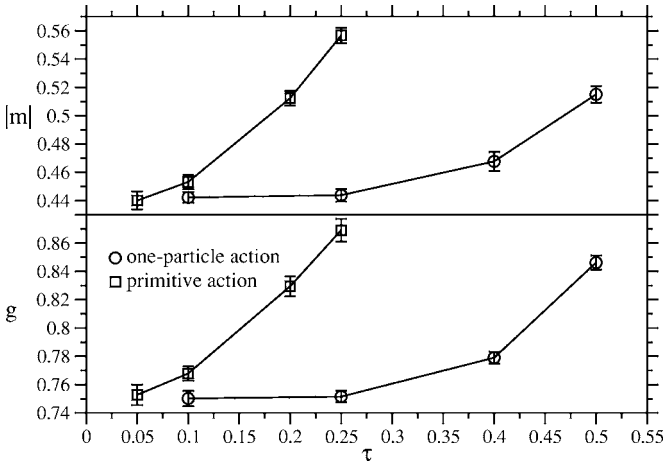

FIG. 4. The magnetization $\langle|m|\rangle$ and its fourth-order cumulant g, calculated by using the one-particle density matrix and the primitive approximation. The model parameters are $V_0=1$ and $J=0.56$ for a system size $L=32$ at temperature $\beta=16$. The values obtained from both methods are compatible in the small-τ limit.

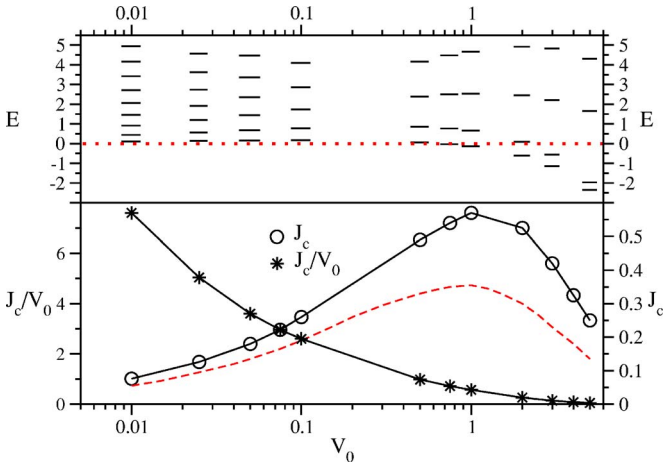

FIG. 5. (Color online) Lower panel: the phase diagram of the coupled double-well chain: the critical ratio J_c/V_0 as well as the critical interaction J_c as functions of the depth of the potential well V_0; the ordered phase is located above the curves and the disordered phase is below the curves. The critical J_c obtained by the mean-field approach is indicated by the dashed line. Upper panel: the low-lying energy eigenvalues of the one-particle Hamiltonian for various V_0, determined by numerical solutions of the Schrödinger equation. The dotted line at $E=0$ indicates the top of the potential barrier.

particle density matrix with $\tau=0.25$, and the spacing between neighboring points within $[x_{\min},x_{\max}]$ was chosen to be 0.01. In all cases studied we used a wide interval of $[x_{\min},x_{\max}]$—e.g., $[-10,+10]$ for $V_0=3$—for the iterative integrations and then truncated this interval to a smaller one while storing into the look-up table for PIMC simulations. The appropriate values for the interval $[x_{\min},x_{\max}]$ in the look-up table were justified by doing a short run of the PIMC simulation to check whether the particles would move beyond the chosen boundaries.

In Fig. 5 we present the zero-temperature phase diagram, in which the critical value J_c is estimated by the intersection of $g(J)$ curves at a given V_0 for various system sizes (up to $L=64$) with fixed aspect ratio $L/\beta=2$. We note the lack of monotonicity of the critical J_c with respect to the potential barrier V_0; J_c decreases with V_0 in the deep-well region, while it increases with V_0 in the small-V_0 region. This nonmonotonic behavior of $J_c(V_0)$ is qualitatively reproduced within the mean-field approximation: Consider the effective single-site Hamiltonian including a mean-field term

$$\mathcal{H}_{\mathrm{mf}}=\frac{p^2}{2}+V_0(x^4-2x^2)-2Jxm, \tag{18}$$

where the order parameter m is the expectation value of the displacement x in the ground state $\psi_0(x,m)$ of $\mathcal{H}_{\mathrm{mf}}$ and is determined self-consistently via

$$m=\int dx x|\psi_0(x,m)|^2. \tag{19}$$

Varying J and solving the nonlinear equation (19) for m numerically, the critical point can be estimated as the value of J above which a nonzero solution exists.

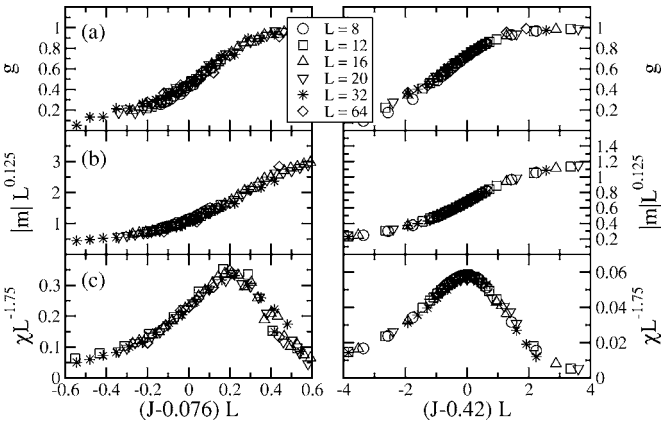

FIG. 6. Scaling plots of the cumulant (a), the magnetization (b), and the susceptibility (c) for $V_0=0.01$ (left) and $V_0=3$ (right) using the two-dimensional Ising universality.

The mean-field result for J_c, depicted in Fig. 5, shows the same nonmonotonic behavior as our results for J_c from the PIMC simulation and has a maximum at $V_0=1$. This behavior of J_c can be understood as follows: In the region $V_0 \gg 1$ the potential has two deep minima separated by a barrier V_0 giving rise to a nearly degenerated ground-state doublet that is well separated from the rest of the spectrum, as shown in the upper panel of Fig. 5. This is called the order-disorder limit [3,10] in the interacting double-well model. The energy difference between the ground state and the first excited state—i.e., the tunneling splitting Γ—is reduced as V_0 grows, which results in a decrease of the critical ordering term J_c. In the region $V_0 \ll 1$, on the other hand, the potential has two shallow minima and the two lowest energy levels are not well separated from the rest of the spectrum. This is called the displacive regime [11] in the interacting double-well model. In this displacive region, the zero-point energy of a single particle lies above the barrier of the local potential so that the local potential is effectively in a single-well form. Without the interaction term, the particles fluctuate around the $x=0$ position (cf. Fig. 3); switching on the interaction shifts the displacement expectation value $\langle x \rangle$ away from the origin, and at the critical coupling J_c the systems undergoes a displacive transition from a symmetric (disordered) phase to a broken symmetry (ordered) phase. The key factor for the strength of the critical displacing force J_c in this case is the width of the local potential, which decreases with increasing V_0: the wider the local potential, the weaker the force J needed for the displacement. Therefore, the critical value J_c increases with V_0 in the displacive regime.

For a particular value of V_0 we can use the scaling form given in Eq. (17) for g, $|m|$, and χ to extract values of the critical exponents. In all cases a good data collapse is achieved with the exponents $\beta_m=1/8, \gamma=7/4$, and $\nu=1.0$, which is representative of the classical 2D Ising universality class. In Fig. 6 we show the finite-size scaling plots for $V_0=3$ and $V_0=0.01$. For $V_0=0.01$, which is well inside the displacive regime, the quality of the scaling decreases and corrections to scaling become more pronounced. Interestingly, the peak of the scaling function $\tilde{\chi}(t)$ of the susceptibility is shifted away from $t=0$ for $V_0=0.01$, whereas it is at $t=0$ for $V_0=3$, indicating the nonuniversality of the scaling function. Our results for $V_0 \ll 1$ indicate that the model is in the Ising universality class even in the displacive regime. For the interaction in the form given in Eq. (14), we expect that a phase transition in the same universality still occurs when the local potential is reduced to only a quartic term. To provide support for this we carried out simulations for the model with a local potential given by $U(x)=x^4$ which exhibits a single well. Our results depicted in Fig. 7 suggest that the critical behavior of this one-well model is indeed consistent with 2D Ising universality [12]. We note that the coupling term (14) that we use can be brought into a form that is more reminiscent of a lattice version of the standard ϕ^4 (quantum) field theory:

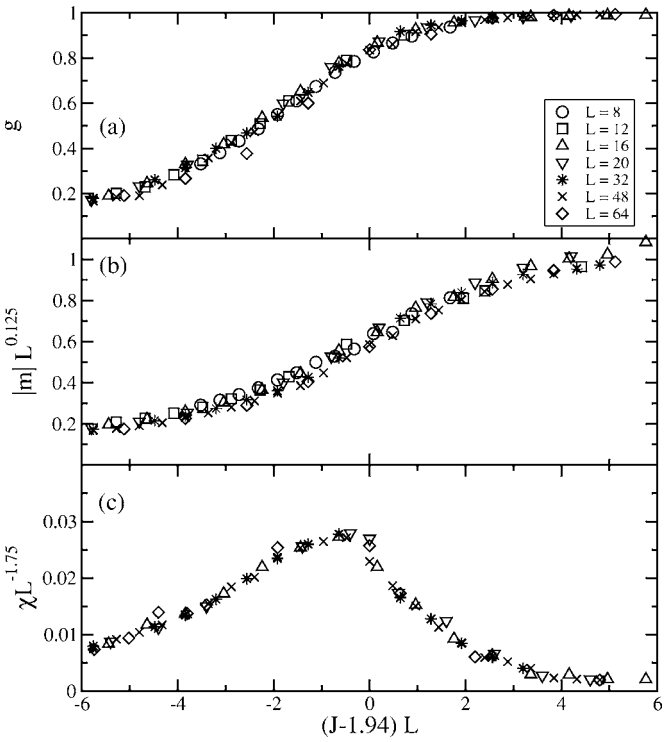

FIG. 7. Scaling plots of the cumulant (a), the magnetization (b), and the susceptibility (c) for the single-well model with $U(x)=x^4$ using the two-dimensional Ising universality. In the scaling plot (c), the system sizes only range from $L=16$ to $L=64$.

$$\mathcal{H}_B = \frac{J}{2}\sum_{i=1}^{L}(x_i - x_{i+1})^2 - J\sum_{i=1}^{L} x_i^2. \tag{20}$$

Together with the local potential (15) this implies that the corresponding continuum model for a scalar field ϕ contains a $(d\phi/dx)^2$ term and a potential energy of the form $V_0[\phi^4 - (2+J/V_0)\phi^2]$. Since J is always positive and can be made arbitrarily large, this model has always a phase transition (at zero temperature). On the other hand, the field theory with a potential energy that has only a single minimum, like the pure quartic potential $V_0\phi^4$, does *not* have a phase transition. We checked, within mean-field as well as with PIMC simulations, that the corresponding lattice model

$$\mathcal{H} = \sum_{i=1}^{L} \left\{ \frac{p_i^2}{2m} + \frac{J}{2}(x_i - x_{i+1})^2 + V_0 x_i^4 \right\} \tag{21}$$

also does not have a phase transition.

To summarize, we have demonstrated that the PIMC within the one-particle density matrix approximation is an efficient method to simulate quantum interacting many-body systems, in which particles are confined to a local potential and interact with each other. Using this method we have studied the zero-temperature phase transition of the coupled double-well chain, both in the order-disorder case, corresponding to a coupled two-level tunneling system, and in the displacive regime, in which the interaction dominates over the double-well structure. Based on this numerical scheme, our further study will include the double-well model coupled through long-range and random interactions and coupled to a dissipative bath [13,14]. In the presence of quenched disorder in the coupling, even for the case without dissipation, implementation of many improved PIMC methods—e.g., Fourier PIMC techniques or cluster algorithms—becomes complex and the computational efficiency reduces. This motivates the choice of a method which provides easy performance and can be extended to the random case in a straightforward way, as the technique applied in this paper does.

[1] P. W. Anderson, B. Halperin, and S. Varma, Philos. Mag. **25**, 1 (1972); W. A. Phillips, J. Low Temp. Phys. **7**, 351 (1972).
[2] W. Arnold and S. Hunklinger, Solid State Commun. **17**, 883 (1975); X. Liu, P. D. Vu, R. O. Pohl, F. Schiettekatte, and S. Roorda, Phys. Rev. Lett. **81**, 3171 (1998).
[3] A. D. Bruce, Adv. Phys. **29**, 111 (1980).
[4] D. M. Ceperley, Rev. Mod. Phys. **67**, 279 (1995).
[5] A. D. Klemm and R. G. Storer, Aust. J. Phys. **26**, 43 (1973); D. Thirumalai, E. J. Bruskin, and B. J. Berne, J. Chem. Phys. **79**, 5063 (1983).
[6] K. E. Schmidt and M. A. Lee, Phys. Rev. E **51**, 5495 (1995); A. N. Drozdov and J. J. Brey, *ibid.* **57**, 1284 (1998).
[7] T. Schneider and E. Stoll, Phys. Rev. B **13**, 1216 (1976).
[8] A. Milchev, D. W. Heermann, and K. Binder, J. Stat. Phys. **44**, 749 (1986).
[9] S. Sachdev, *Quantum Phase Transitions* (Cambridge University Press, Cambridge, England, 1999).
[10] A. N. Rubtsov and T. Janssen, Phys. Rev. B **63**, 172101 (2001).
[11] In some literature on the classical ϕ^4 model the displacive region is defined as the region where the local potential exhibits a single well (see, e.g., [7,8]). In this paper we use the term for the low-barrier region in our quantum model.
[12] M. Barma and M. E. Fisher, Phys. Rev. Lett. **53**, 1935 (1984); A. D. Bruce, J. Phys. A **18**, L873 (1985).
[13] L. Capriotti, A. Cuccoli, A. Fubini, V. Tognetti, and R. Vaia, Europhys. Lett. **58**, 155 (2002).
[14] T. Matsuo, Y. Natsume, and T. Kato, J. Phys. Soc. Jpn. **75**, 103002 (2006).